

EUR Research Information Portal

Population pharmacokinetics of nadroparin for thromboprophylaxis in COVID-19 intensive care unit patients

Published in:

British Journal of Clinical Pharmacology

Publication status and date:

Published: 01/05/2023

DOI (link to publisher):

[10.1111/bcp.15634](https://doi.org/10.1111/bcp.15634)

Document Version

Publisher's PDF, also known as Version of record

Document License/Available under:

CC BY-NC-ND

Citation for the published version (APA):

Romano, L. G. R., Hunfeld, N. G. M., Kruij, M. J. H. A., Endeman, H., & Preijers, T. (2023). Population pharmacokinetics of nadroparin for thromboprophylaxis in COVID-19 intensive care unit patients. *British Journal of Clinical Pharmacology*, 89(5), 1617-1628. <https://doi.org/10.1111/bcp.15634>

[Link to publication on the EUR Research Information Portal](#)

Terms and Conditions of Use

Except as permitted by the applicable copyright law, you may not reproduce or make this material available to any third party without the prior written permission from the copyright holder(s). Copyright law allows the following uses of this material without prior permission:

- you may download, save and print a copy of this material for your personal use only;
- you may share the EUR portal link to this material.


In case the material is published with an open access license (e.g. a Creative Commons (CC) license), other uses may be allowed. Please check the terms and conditions of the specific license.

Take-down policy

If you believe that this material infringes your copyright and/or any other intellectual property rights, you may request its removal by contacting us at the following email address: openaccess.library@eur.nl. Please provide us with all the relevant information, including the reasons why you believe any of your rights have been infringed. In case of a legitimate complaint, we will make the material inaccessible and/or remove it from the website.

ORIGINAL ARTICLE

Population pharmacokinetics of nadroparin for thromboprophylaxis in COVID-19 intensive care unit patients

Lorenzo G. R. Romano¹  | Nicole G. M. Hunfeld^{2,3}  | Marieke J. H. A. Kruij¹  |
Henrik Endeman³ | Tim Preijers^{2,4} 

¹Department of Hematology, Erasmus MC, Erasmus University Medical Center Rotterdam, Rotterdam, The Netherlands

²Department of Hospital Pharmacy, Erasmus MC, Erasmus University Medical Center Rotterdam, Rotterdam, The Netherlands

³Department of Intensive Care, Erasmus MC, Erasmus University Medical Center Rotterdam, Rotterdam, The Netherlands

⁴Rotterdam Clinical Pharmacometrics Group, Rotterdam, The Netherlands

Correspondence

Lorenzo G. R. Romano, Erasmus University Medical Center, Wytemaweg 80, 3015 CN Rotterdam, The Netherlands.
Email: l.romano@erasmusmc.nl

Funding information

No funding was obtained for this study.

Aims: Nadroparin is administered to COVID-19 intensive care unit (ICU) patients as thromboprophylaxis. Despite existing population pharmacokinetic (PK) models for nadroparin in literature, the population PK of nadroparin in COVID-19 ICU patients is unknown. Moreover, optimal dosing regimens achieving anti-Xa target levels (0.3–0.7 IU/mL) are unknown. Therefore, a population PK analysis was conducted to investigate different dosing regimens of nadroparin in COVID-19 ICU patients.

Methods: Anti-Xa levels ($n = 280$) from COVID-19 ICU patients ($n = 65$) receiving twice daily (BID) 5700 IU of subcutaneous nadroparin were collected to perform a population PK analysis with NONMEM v7.4.1. Using Monte Carlo simulations ($n = 1000$), predefined dosing regimens were evaluated.

Results: A 1-compartment model with an absorption compartment adequately described the measured anti-Xa levels with interindividual variability estimated for clearance (CL). Inflammation parameters C-reactive protein, D-dimer and estimated glomerular filtration rate based on the Chronic Kidney Disease Epidemiology Collaboration equation allowed to explain the interindividual variability of CL. Moreover, CL was decreased in patients receiving corticosteroids (22.5%) and vasopressors (25.1%). Monte Carlo simulations demonstrated that 5700 IU BID was the most optimal dosing regimen of the simulated regimens for achieving prespecified steady-state $t = 4$ h anti-Xa levels with 56.7% on target (0.3–0.7 IU/mL).

Conclusion: In our study, clearance of nadroparin is associated with an increase in inflammation parameters, use of corticosteroids, vasopression and renal clearance in critically ill patients. Furthermore, of the simulated regimens, targeted anti-Xa levels were most adequately achieved with a dosing regimen of 5700 IU BID. Future studies are needed to elucidate the underlying mechanisms of found covariate relationships.

KEYWORDS

critical care, haematology, infectious diseases, intensive care, pharmacodynamics, pharmacokinetics, modelling and simulation, thrombosis

The authors confirm that the Principal Investigator for this paper is Nicole G. M. Hunfeld, PharmD, PhD.

This is an open access article under the terms of the [Creative Commons Attribution-NonCommercial-NoDerivs](https://creativecommons.org/licenses/by-nc-nd/4.0/) License, which permits use and distribution in any medium, provided the original work is properly cited, the use is non-commercial and no modifications or adaptations are made.

© 2022 The Authors. *British Journal of Clinical Pharmacology* published by John Wiley & Sons Ltd on behalf of British Pharmacological Society.

1 | INTRODUCTION

In late 2019, coronavirus disease 2019 (COVID-19) resulted in a major rise in patients requiring hospitalization and admission to the intensive care unit (ICU). COVID-19 is characterized by (severe) respiratory symptoms and other complications including a hypercoagulable state characterized by high D-dimers, fibrinogen and von Willebrand factor levels.¹⁻³ Furthermore, an increased incidence of thrombo-embolic events has been described in critically ill COVID-19 ICU patients.^{2,4-7} Despite new treatment modalities (e.g., dexamethasone), the incidence of thrombo-embolic events in hospitalized COVID-19 patients remains high.⁸

In response, international guidelines by the International Society for Thrombosis and Hemostasis have advised the administration of parenteral anticoagulants.⁹ However, adequate dosing of low molecular weight heparins (LMWHs) in COVID-19 patients is challenging. First, COVID-19-related coagulopathy is associated with high levels of procoagulant factors, associated with thrombosis and subsequent multiorgan injury.^{10,11} Second, disease pathophysiology could influence the individual patient's pharmacokinetic (PK) parameters, such as clearance (CL) and volume of distribution (Vd): Changes in renal function, microvascular failure (by coagulopathy and endothelial dysfunction) and organ dysfunction have been reported in critically ill COVID-19 patients, which are known to influence PK parameters in other infectious diseases.^{1,11-13} Moreover, vasopressor use has been associated with lower levels of anti-Xa.¹⁴ In addition, the phenomenon of augmented renal clearance also has been suggested in COVID-19 patients with high inflammation.¹⁵⁻¹⁷

Despite multiple randomized controlled trials, optimal dose regimens in order to achieve prespecified anti-Xa levels for prophylactic treatment are unknown.^{18,19} However, no additional benefit was obtained using therapeutic doses vs. prophylactic doses of nadroparin. Moreover, to adequately interpret if prespecified anti-Xa target levels are met, multiple guidelines advise anti-Xa sampling at 4 h (at peak level) after LMWH administration.^{20,21} In clinical practice, especially in ICU care, respecting specific sample timing can be challenging.

In population PK analyses, covariate relationships can be associated with PK parameters and their effect can be quantified.²² Moreover, such studies allow the evaluation of optimal dosing and sampling strategies. Furthermore, a validated population PK model can also be applied to perform dose individualization based on measurements taken from clinical routine practice.²³

Previously, a population PK model describing anti-Xa levels after administration of nadroparin was developed for morbidly obese bariatric surgery patients and paediatric open heart surgery patients.^{24,25} As no population PK analyses have yet been conducted in COVID-19 ICU patients for nadroparin, the objective of this study was to assess different nadroparin dosing regimens by constructing a population PK model using anti-Xa levels obtained in critically ill ICU COVID-19 patients.

What is already known about this subject

- Population pharmacokinetics (PK) of nadroparin has only been described in morbidly obese bariatric surgery patients and paediatric patients undergoing open heart surgery and not in COVID-19 intensive care unit patients.
- Previous studies in COVID-19 intensive care unit patients demonstrated that the clearance of other low molecular weight heparins was mainly associated with serum creatinine or creatinine clearance and the volume of distribution to body weight.

What this study adds

- Using a population PK analysis, it was demonstrated that increasing inflammation parameters are associated with increased values for clearance.
- Using the constructed population PK model, the adequacy of the 5700 IU twice daily dosing regimen to achieve anti-Xa levels between 0.3 and 0.7 IU/mL was demonstrated.

2 | METHODS

2.1 | Patient population and clinical data

A single-centre observational retrospective cohort study was performed collecting data from ICU patients with at least 1 positive polymerase chain reaction test for SARS-CoV-2 during hospitalization. Data were collected for the complete duration of ICU admission until discharge to the ward or death between 1 March 2020 and 30 January 2021 in 2 phases. Patients from the first phase all served for the modelling cohort, whereas patients in the second phase were admitted after 1 September and randomly included for either the model cohort or the validation cohort. Patients were excluded if therapeutic doses of nadroparin were applied or if a thrombotic event had occurred while being transferred to the ICU.

All patients were treated according to the local ICU protocol with nadroparin 5700 IU twice daily (BID) subcutaneously, also in case of renal replacement therapy. In case of dalteparin use prior to admission, measurements were excluded for at least 24 h after the last dalteparin administration. In case of estimated glomerular filtration rate based on the Chronic Kidney Disease Epidemiology Collaboration equation (CKD-EPI-eGFR) <30 mL/min, the nadroparin dosing frequency was lowered in consultation with the critical care pharmacist. The medical research ethics committee of the Erasmus University Medical Center approved the study and waived informed consent

requirement, given that all data acquired for this study were part of usual care (MEC 2020-0381).

Vasopressor (including inodilators) use comprised application of norepinephrine, epinephrine or enoximone. Renal replacement therapy consisted of continuous venovenous haemofiltration dialysis or filtration. For administration of corticosteroids, (methyl)prednis (ol)one or dexamethasone were applied. CKD-EPI-eGFR was calculated using serum creatinine, age and sex, according to the Dutch multidisciplinary guideline for chronic kidney injury.²⁶

2.2 | Sampling and measurement of anti-Xa levels

ICU personnel were instructed to measure anti-Xa levels 4 h after nadroparin administration, twice a week (prespecified target in ICU protocol: 0.3–0.7 IU/mL). The anti-Xa levels were measured using a Sysmex CS-5100 System™ (Siemens Healthcare Diagnostics, Erlangen, Germany) which applied colour detection after an enzymatic reaction according to the instructions of the manufacturer. This system had a lower limit of quantification of 0.1 IU/mL and an upper limit of quantification of 4.0 IU/mL.

2.3 | Population PK analysis

Nonlinear mixed effect modelling was applied in order to develop a population PK model describing the measured anti-Xa levels vs. time curves. Model development was conducted using NONMEM v7.4 (ICON Development Solutions, Ellicott City, MD, USA) and was guided using Perl-speaks-NONMEM (PsN) v4.7.0, whereas Pirana v2.9.9 was used for model management.²⁷ Because the method for optimal inclusion (M3-method²⁸) of the anti-Xa measurements below the limit of quantification (BLQ < 0.1 IU/mL) was used, second-order conditional estimation with the Laplace method was applied with epsilon–eta interaction.²⁹ Data management and graphical model diagnostics were performed using R v4.0.1 (R Core Team, 2020) and Xpose v4.7.0.^{30,31}

2.4 | Model development

As a previously published population PK model was available in the literature established using data from 28 morbidly obese and 7 nonobese patients receiving nadroparin for surgery, it was first evaluated if this model allowed to describe the measured anti-Xa levels from the present cohort.²⁵ This model consisted of 2 disposition compartments, a transit compartment and an absorption compartment. Consecutively, the population PK parameter values from the published model were used as initial values for the start of the present model construction. Furthermore, it was evaluated whether including 1 or multiple transit compartments was of additional value.

Model construction was conducted using a stepwise procedure, in which first a structural model was established and, subsequently, the statistics were evaluated. For the statistical model, interindividual

variability (IIV) was evaluated for the population parameters and described using a log-normal distribution. Estimation of interoccasion variability was not evaluated as the number of dosing occasions differed between patients. To estimate the residual unexplained variability (RUV), an additive, proportional or a combined residual error model was evaluated.

To evaluate the ability of 2 nested models to describe the measured anti-Xa levels, the difference in the objective function value (dOFV) was applied. As the latter value is χ^2 distributed, values >3.84 and 5.99 indicate a significant difference of $P < .05$ for 1 or 2 degrees of freedom, respectively.

2.5 | Covariate analysis

After establishing the structural and statistical model, patient and pathophysiological characteristics were used to explain the IIV and RUV using covariate relationships.³² Covariates were selected for evaluation if their physiological or biological association with a specific parameter was plausible, in case of earlier established effects on nadroparin or LMWH clearance, including factors related to renal function (or failure) in population PK models (ideal/lean body weight, length, BMI, creatinine, urea, sex, eGFR, vasopressin use, use of dialysis and arterial lactate), possible covariates related to inflammation (C-reactive protein [CRP], ferritin, leucocytes, lymphocytes, neutrophils, IL-6 and corticosteroid use) influencing augmented renal clearance and/or other organ dysfunction, such as hepatic function (albumin, alanine transaminase and bilirubin) and coagulopathy (thrombocytes, blood group, fibrinogen and D-dimer). In case of a continuous covariate, the following relationships (linear, power and exponential) were evaluated:

$$\theta_{TV} = \theta_{Pop} * (1 + \theta_{Cov} * (COV - COV_{med})),$$

$$\theta_{TV} = \theta_{Pop} * \left(\frac{COV}{COV_{med}} \right)^{\theta_{Cov}},$$

$$\theta_{TV} = \theta_{Pop} * e^{(\theta_{Cov} * (COV - COV_{med}))},$$

in which θ_{TV} is the typical value of the PK parameter, θ_{Pop} is the population PK parameter, θ_{Cov} is the fraction of the population PK parameter for the covariate value described by COV and its median (COV_{med}). For the evaluation of dichotomous relationships, the following equation was applied:

$$\theta_{TV} = \theta_{Pop} * \theta_{Cov}^{COV},$$

in which the value for COV is 1 if the relationship was present and 0 otherwise. The covariate analysis was conducted using a forward inclusion and backwards elimination procedure by selecting covariate relationships that resulted in a dOFV of >3.84 ($P < .05$, $df = 1$) and >6.68 ($P < .01$, $df = 1$), respectively. The collinearity of all continuous covariates was assessed using a correlation matrix to evaluate whether such covariate relationships could be associated with the same PK parameter.

2.6 | Model evaluation

To verify whether the constructed population PK model sufficiently described the measured anti-Xa levels, goodness-of-fit (GOF) plots were obtained.³³ Model diagnostics were also performed using prediction-corrected visual predictive checks (pdVPCs) applied by Monte Carlo simulation of 2000 anti-Xa level vs. time curves using the final model.³⁴ Similarly, as a means of internal validation, a pdVPC and a GOF plot were used to evaluate the ability of the final model to describe the measured anti-Xa levels for the validation cohort. Furthermore, the robustness of the parameter estimates from the final model was verified using a nonparametric bootstrap analysis with 2000 replications.

2.7 | Dosing regimen simulations

To evaluate whether different nadroparin dosing regimens allow to adequately achieve the prespecified anti-Xa target level ranges, maximum a posteriori Bayesian analysis using the final model was conducted. With maximum a posteriori Bayesian analysis, empirical Bayesian estimates can be obtained for the model parameters for which IIV has been associated and can be used to calculate the individual PK parameter values. Using these parameter values, the steady-state anti-Xa levels at $t = 4$ h were calculated for different predefined dosing regimens for the modelling and the validation cohort.

To inspect the influence of the covariate relationships from the final model on the predefined nadroparin dosing regimens, Monte Carlo simulations ($n=1000$) were conducted.³⁵ Monte Carlo simulations allow taking the covariate relationships into account when values for the individual PK parameters are simulated. The values used for covariate relationships were simulated uniformly between the corresponding minimal and maximal values from the total population. Correlations between the covariate relationships were not taken into account as such relationships cannot be associated with the same model parameter. During Monte Carlo simulation, only values were generated for the parameters that have been associated with IIV. As a result, individual PK parameters are obtained, which were used to calculate the steady-state $t = 4$ h anti-Xa levels for different predefined dosing regimens.

To assess the influence of the covariate values, 2 scenarios were simulated. First, all covariate values were taken into account for calculating the steady-state anti-Xa levels for each dosing regimen. Second, the simulated values for the covariate relationships were taken into account for 1 covariate relationship at a time. In this situation, when a single covariate relationship was evaluated, the other covariate values were set to the median in case of the continuous covariates and to zero in case of a dichotomous relationship.

Additionally, for assessing the influence of the continuous covariate values, different scenarios were simulated to evaluate which nadroparin dosing regimen would achieve a predicted anti-Xa level of 0.4 IU/mL for the corresponding covariate relationship.

3 | RESULTS

3.1 | Patient population

First, 65 critically ill ICU patients with COVID-19 were enrolled for the model construction. A second cohort with another 25 patients served as a validation cohort. Table 1 shows the collected patient and pathophysiological characteristics as well as the number of doses and times of anti-Xa level measurement.

3.2 | Population PK modelling

The ability of a previously published model to describe the measured anti-Xa levels from the modelling cohort was evaluated. In Figure S1, the GOF plots are shown. As the model was not able to describe the obtained data adequately, model construction was initiated using a 2 disposition compartment model with an absorption compartment. Addition of a transit compartment did not result in a better prediction of the anti-Xa levels and was, therefore, omitted. Adding a baseline parameter was not evaluated, as no physiological evidence was available for the investigated population.

Table 2 presents the parameter estimates from the structural model. For all parameter estimates, the precision was high as the values ranged from 7 to 12% except for the RUV (33%). For the structural model, the RUV was most adequately described by an additive error solely. IIV was obtained for CL only. Inclusion of additional compartments did not result in a better model ($dOFV = 0.003$; $P = .96$). Moreover, shrinkage values for the IIV on CL (12%) and the RUV (13%) were low, indicating that there were sufficient data to estimate these parameters. Table 2 shows the final model with all remaining covariate relationships after the backwards elimination procedure. With rising values for CRP, D-dimer and CKD-EPI-eGFR, the CL also increased. Furthermore, with corticosteroid or vasopressor use, CL was decreased by 22.5% and 25.1%, respectively. Due to the addition of covariate relationships in the final model, the population value of CL increased from 1140 to 2230 mL/h.

After the final model was constructed, the RUV was re-evaluated showing that the proportional error was of additional value ($dOFV = 29.1$, $P < .001$). Therefore, the latter parameter was included in the final model afterwards. Subsequently, the forward inclusion backward elimination procedure was reiterated showing the same covariate relationships. The correlation matrix demonstrated no collinearity between the covariate relationships of the final model (Figure S2). The control stream for the final model was added to Appendix SA.

3.3 | Model evaluation

In Figure 1, the GOF plots depict that the model was able to adequately predict the anti-Xa levels for the modelling cohort. In Figure 1A, the highest population predicted anti-Xa levels show a

TABLE 1 General characteristics of the study population

| | Total population No. (%) or median [IQR] | Validation cohort No. (%) or median [IQR] | Modelling cohort No. (%) or median [IQR] |
|---|---|--|---|
| Patient characteristics | | | |
| Total No. of patients | 90 | 25 | 65 |
| Age (years) | 63.0 [53.0–69.7] | 63.0 [54.0–69.0] | 62.0 [53.0–70.0] |
| SOFA score at first anti-Xa sampling | 6 [4–7] | 5 [3.5–6.5] | 6 [4–8.5] |
| Mechanical ventilation at first anti-Xa sampling | 78 (87) | 21 (84) | 57 (87) |
| Receiving renal replacement therapy ^a | 8 (9) | 2 (8) | 6 (9) |
| Blood group O ^b | 21 (23) | 0 (0) | 21 (32) |
| Height (m) | 1.75 [1.65–1.80] | 1.75 [1.67–1.80] | 1.75 [1.65–1.80] |
| Bodyweight (kg) | 89.0 [78.5–97.3] | 89.0 [81.0–96.0] | 89.0 [78.0–100] |
| Body mass index (kg/m ²) | 29.6 [27.5–32.3] | 29.6 [27.5–32.1] | 29.7 [27.5–32.3] |
| Lean body mass calculated (kg) | 60.7 [50.0–67.3] | 63.8 [52.2–67.3] | 57.8 [49.9–67.3] |
| Albumin (g/L) | 20.0 [18.5–23.0] ^c | - | 20.0 [18.5–23.0] |
| Alanine transaminase (U/L) | 49.5 [32.0–81.0] ^c | - | 49.5 [32.0–81.0] |
| Bilirubin (μmol/L) | 6.00 [4.00–7.25] ^c | - | 6.00 [4.00–7.25] |
| Ferritin (μg/L) | 913 [544–1314] ^c | - | 913 [544–1314] |
| Thrombocytes (10 ⁹ /L) | 345 [265–417] ^c | - | 345 [265–417] |
| Leucocytes (10 ⁹ /L) | 10.3 [8.80–12.3] ^c | - | 10.3 [8.80–12.3] |
| Fibrinogen (10 ⁹ /L) | 6.00 [4.90–6.70] ^c | - | 6.00 [4.90–6.70] |
| D-dimer (mg/L) | 1.24 [0.85–2.18] | 1.06 [0.57–2.13] | 1.29 [0.87–2.19] |
| Using vasopressors at start | 77 (86) | 19 (76) | 58 (89) |
| Using corticosteroids at start | 64 (71) | 22 (88) | 42 (65) |
| Absolute neutrophil count (10 ⁹ /L) | 7.80 [6.21–9.38] ^c | - | 7.80 [6.21–9.38] |
| Absolute lymphocyte count (10 ⁹ /L) | 1.10 [0.72–1.52] ^c | - | 1.10 [0.72–1.52] |
| IL-6 (pg/mL) | 30.5 [14.5–57.0] ^c | - | 30.5 [14.5–57.0] |
| CRP (mg/L) | 61.0 [32.5–101] | 55.0 [32.5–62.0] | 76.0 [35.5–124] |
| Arterial lactate (mmol/L) | 1.15 [1.00–1.40] ^c | - | 1.15 [1.00–1.40] |
| eGFR based on CKD-EPI (mL/min) | 93.2 [76.0–109] | 91.5 [75.9–108] | 94.4 [78.6–111] |
| Comorbidities/possible influencing factors | | | |
| Diabetes mellitus type 2 | 30 (33) | 6 (24) | 24 (37) |
| Acute kidney failure | 7 (8) | 0 (0) | 7 (11) |
| Liver cirrhosis | 2 (2) | 0 (0) | 2 (3) |
| Hypertension | 43 (48) | 10 (40) | 33 (51) |
| Asthma or COPD | 14 (16) | 2 (8) | 12 (18) |
| Oncological | 6 (7) | 1 (4) | 5 (8) |
| Miscellaneous ^d | 6 (1) | 2 (0) | 4 (2) |
| Pharmacokinetic data | | | |
| Total number of observations | 427 | 147 | 280 |
| No. of observations per individual | 4 [2–6] | 5 [2–9] | 4 [2–5] |
| Number of BLQ samples | 33 (7.7) | 12 (8.2) | 21 (7.5) |
| No. of observations Day 1 (>0–12 h) | 288 (67) | 115 (73) | 173 (64) |
| No. of observations Day 2 (>12–36 h) | 127 (30) | 30 (22) | 97 (29) |
| No. of observations Day 3 (>36–72 h) | 10 (2) | 1 (2) | 9 (2) |

All continuous patient characteristics, except for age, height and sequential organ failure assessment (SOFA) score at first anti-Xa sampling, were calculated using multiple values from each individual, which were used to calculate the median values to present in this table.

BLQ, below limit of quantification; CKD-EPI, Chronic Kidney Disease Epidemiology Collaboration equation; COPD, chronic obstructive pulmonary disease; CRP, C-reactive protein; eGFR, estimated glomerular filtration rate; IL, interleukin.

^aPeripheral haemodialysis, peritoneal dialysis or continuous venovenous haemodialysis.

^bBlood group was unknown for two patients.

^c $n = 65$ (only collected for the modelling cohort).

^dComprising sickle cell disease, pregnancy, inherited bleeding disorder, familial Mediterranean fever, rheumatoid disease and neurological disease.

TABLE 2 Estimated population PK parameters for the structural model, final model and bootstrap analysis

| | Structural model | | | Final model | | | Bootstrap analysis | |
|--|------------------|---------|----------|-------------|---------|----------|--------------------|-------------------|
| | Estimate | RSE (%) | Shr. (%) | Estimate | RSE (%) | Shr. (%) | Estimate | 95% CI |
| Structural model | | | | | | | | |
| Absorption rate (ka ; h^{-1}) | 0.284 | 33 | | 0.276 | 28 | | 0.270 | [0.070–0.483] |
| Clearance (CL; mL/h) | 1140 | 7 | | 2230 | 12 | | 2235.9 | [1686.1–2780.3] |
| Volume of central compartment (Vd; mL) | 10 600 | 12 | | 11 000 | 22 | | 10 757.2 | [7024.7–14 957] |
| Interindividual variability (%CV) | | | | | | | | |
| IIV on CL | 55.1 | 10 | 12 | 34.9 | 21 | 14 | 35.0 | [12.6–48.9] |
| Residual variability | | | | | | | | |
| Additive residual error (IU/mL) | 0.155 | 8 | 13 | 0.086 | 13 | 13 | 0.084 | [0.062–0.110] |
| Proportional residual error (%CV) | - | | | 0.2 | 18 | | 0.19 | [0.14–0.26] |
| Covariate relations | | | | | | | | |
| CL–CRP | - | | | 0.182 | 21 | | 0.183 | [0.112–0.253] |
| CL–D-dimer | - | | | 0.117 | 56 | | 0.122 | [0.007–0.228] |
| CL–use of vasopressors | - | | | 0.749 | 8 | | 0.757 | [0.649–0.848] |
| CL–GFR _{CKD-EPI} | - | | | 0.368 | 33 | | 0.370 | [0.177–0.560] |
| CL–use of corticosteroids | - | | | 0.775 | 11 | | 0.787 | [0.635–0.916] |
| Model characteristics | | | | | | | | |
| Objective function value | –524.9 | | | –670.6 | | | –689.5 | [–849.5 – –491.7] |
| Condition number | 18.3 | | | 207.1 | | | - | |

The presented typical values are obtained for an ICU patient having a CRP level of 100, a D-dimer level of 10 and a GFR of 80 mL/h without receiving corticosteroids or vasopressors.

$$ka \left(h^{-1} \right) = 0.276,$$

$$CL_i \text{ (mL/h)} = 2230 \times \left(\frac{CRP}{100} \right)^{0.182} \times \left(\frac{D-dimer}{10} \right)^{0.117} \times \left(\frac{GFR_{CKD-EPI}}{80} \right)^{0.368} \times 0.749^{Vasopressors} \times 0.775^{Corticosteroids} \times e^{\eta_i},$$

$$Vd \text{ (mL)} = 11,000.$$

In the equation for CL, the η_i represents the random effect for an individual patient, that is, the difference between the typical value for a PK parameter and the value for an individual PK parameter. Moreover, the exponents *Vasopressors* and *Corticosteroids* are both dichotomous variables having a value of 1 if use occurred and 0 otherwise. The bootstrap analysis was conducted using 2000 replicated datasets.

CI, confidence interval as obtained using the 2.5th and 97.5th percentiles from the nonparametric distributions; CL, clearance; CRP, C-reactive protein; CV, coefficient of variation; GFR, glomerular filtration rate based on the Chronic Kidney Disease Epidemiology Collaboration equation; IIV, interindividual variability; PK, pharmacokinetic; RSE, relative standard error; Shr., shrinkage.

slight deviation, which is corrected when the IIV and covariate relationships on CL are taken into account, as shown in Figure 1B. For the targeted anti-Xa levels, the predicted anti-Xa levels were symmetrically distributed around the line of identity ($y = x$). Furthermore, there was no significant bias shown for the RUV of the final model, as the predicted values were symmetrically around the line $y = 0$ and values for the conditional weighted residuals were almost completely between -2 and 2 (Figure 1C,D).

The ability of the model able to adequately describe the anti-Xa levels is demonstrated in the pdVPC from Figure 2, as the 2.5th, 50th

and 97.5th percentile (solid red and blue lines, respectively) of the measured anti-Xa levels were contained within the corresponding red and blue shaded areas, which were obtained by Monte Carlo simulation. However, the 2.5th percentile showed a small deviation, as the value for the second bin was lower than the values obtained for the 5th percentile using simulation. The latter was due to the measured anti-Xa levels of the 2.5th percentile being BLQ at each time point for that bin.

Using a bootstrap analysis with 2000 iterations, the robustness of the final model was evaluated (Table 2). All medians for the parameter estimates were similar to the parameter estimates obtained for the

FIGURE 1 Goodness-of-fit of the plot for the final model

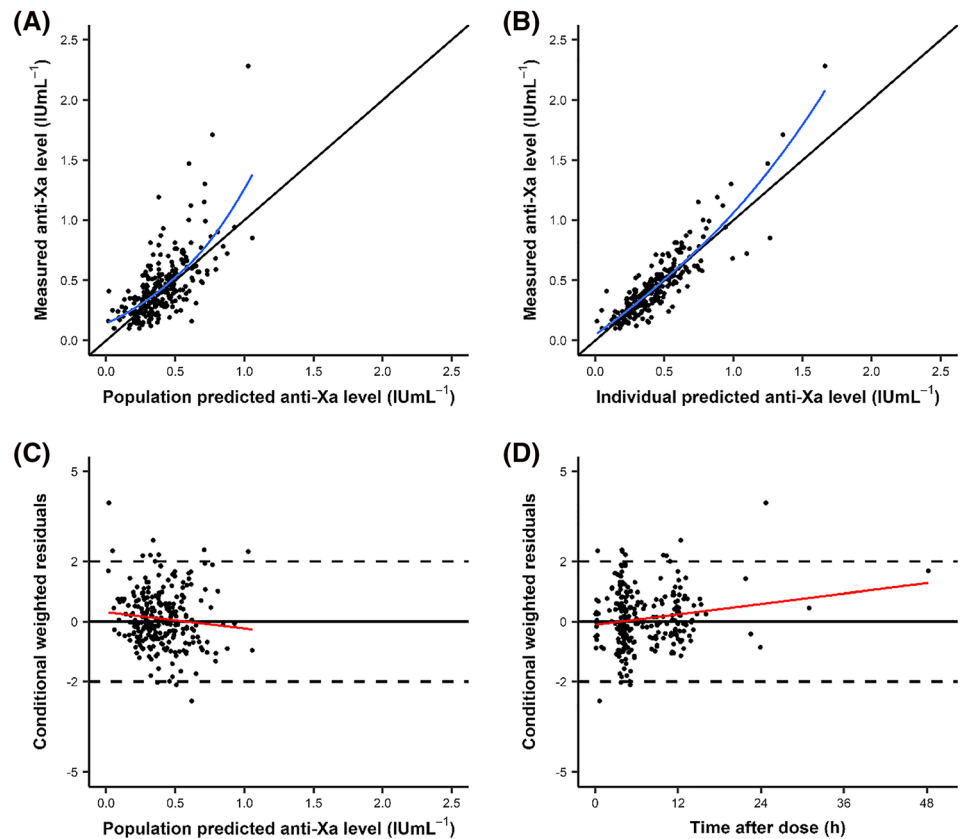
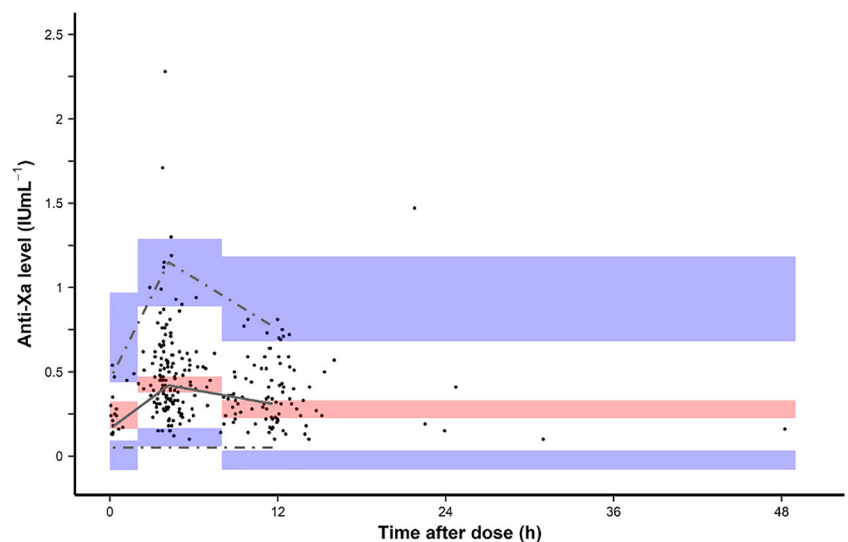


FIGURE 2 Prediction-corrected visual predictive check of the final model



final model. Moreover, the obtained nonparametric confidence intervals showed that all model parameters were adequately estimated.

For the validation cohort, GOF plots (Figure S3) and a pdVPC (Figure 3) showed that the population PK parameters slightly underpredicted the measured anti-Xa levels for the validation cohort (Figure S3A). However, the latter was corrected using IIV on CL, as the measured anti-Xa levels vs. the individual predicted anti-Xa levels were symmetrically distributed surrounding the line of identity ($y = x$; Figure S3B). The pdVPC (Figure 3) for the validation cohort also showed the adequacy of the current model to predict the anti-Xa

levels for the validation cohort. Although, a slight underprediction was also seen for the 50th percentile of the data, as the solid grey line (data) was slightly above the red-shaded areas (model simulations).

3.4 | Predictive performance

When performing Bayesian forecasting and Monte Carlo simulations, individual PK parameter values were obtained for CL solely since only for this parameter IIV was estimated. For the other model parameters,

only the population PK parameter value was taken into account for calculation of the steady-state $t = 4$ h anti-Xa levels.

Using the individual PK parameter values obtained by Bayesian forecasting with the final model, the achieved $t = 4$ h anti-Xa levels

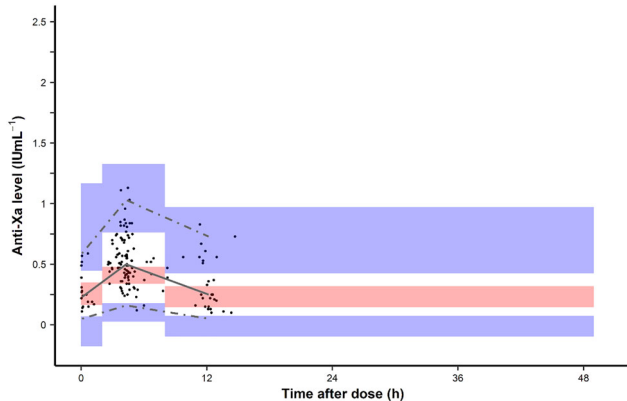


FIGURE 3 Prediction-corrected visual predictive check for the validation cohort using the final model

for the total cohort were calculated and depicted in Figure 4. It was demonstrated that, with a dose of 5700 IU BID, 55.4% of patients from the modelling and 60% of the patients from the validation cohort were within the desired anti-Xa level range. For the validation cohort, most patients (64%) were within the range with 5700 IU once daily. However, a dosing regimen with 5700 IU BID resulted in the highest number of patients (56.7%) within the targeted anti-Xa level range for the total cohort (Figure S4).

In Figure 5, the Monte Carlo simulation of the steady-state $t = 4$ h anti-Xa levels for the different dosing strategies is depicted. For each dosing strategy, it was shown that when all covariate relationships were taken into account, a dosing regimen of 5700 IU BID resulted in the most anti-Xa levels within the anti-Xa target levels range (0.3–0.7 IU/mL). However, for each simulated covariate relationship, the anti-Xa levels were in general above the upper target anti-Xa level (0.7 IU/mL) for the lowest covariate values. The latter was especially the case for the 7600 IU BID dosing regimen, as shown in Figure 5. Similarly, the evaluation of the dichotomous covariate relationships (Figure 6) demonstrated that a dosing regimen of 5700 IU BID and

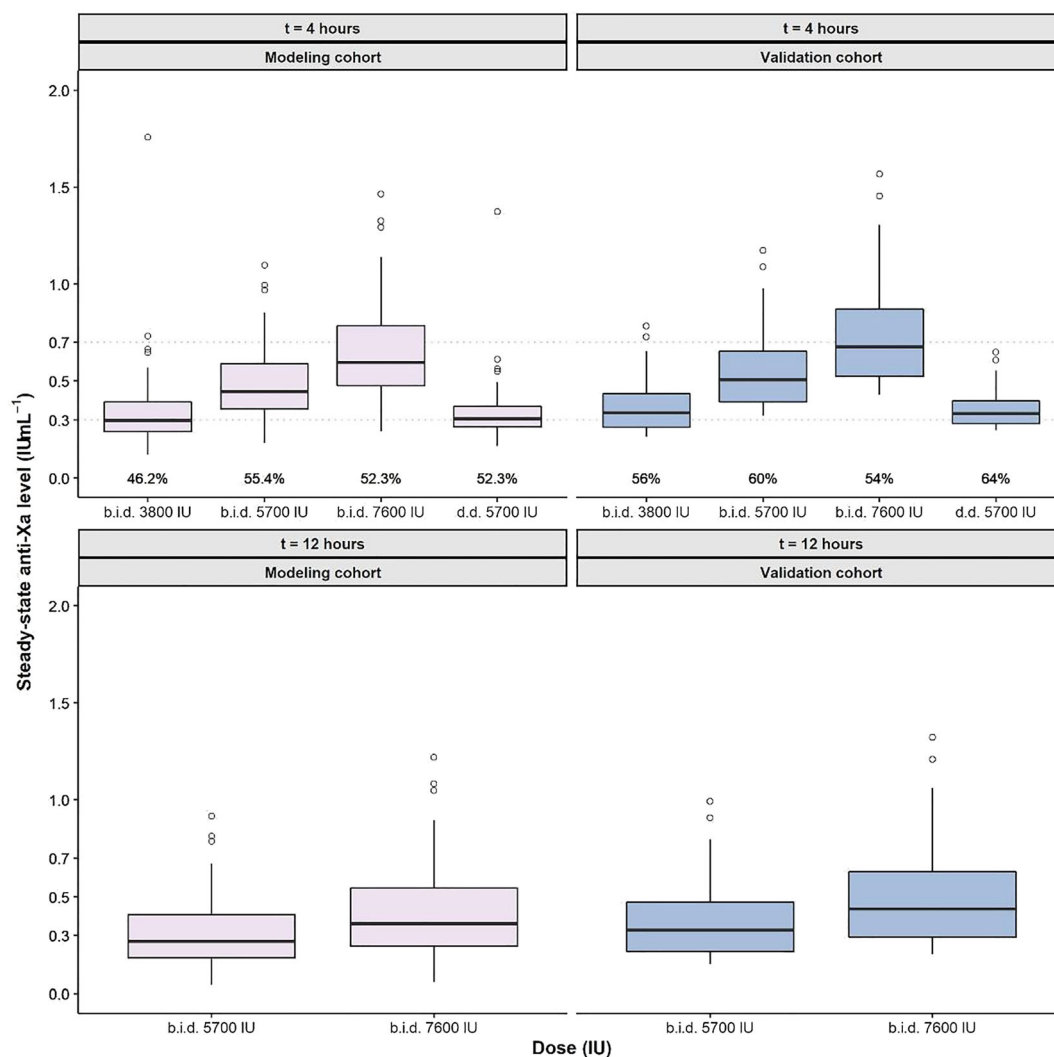


FIGURE 4 Estimated anti-Xa level at 4 and 12 h after dose administration for different dosing regimens

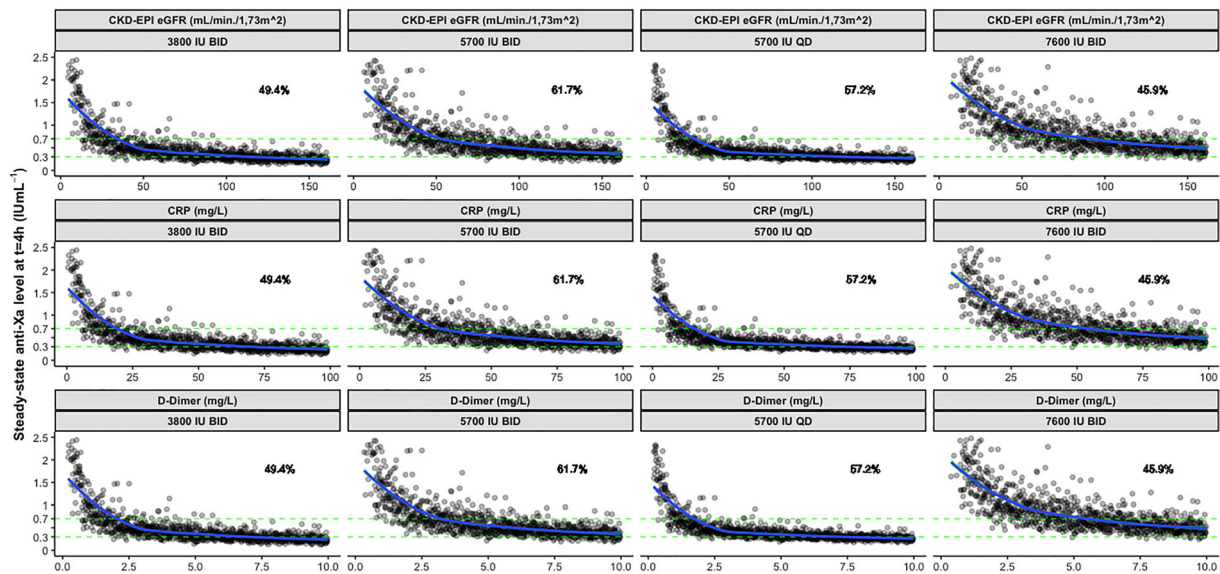
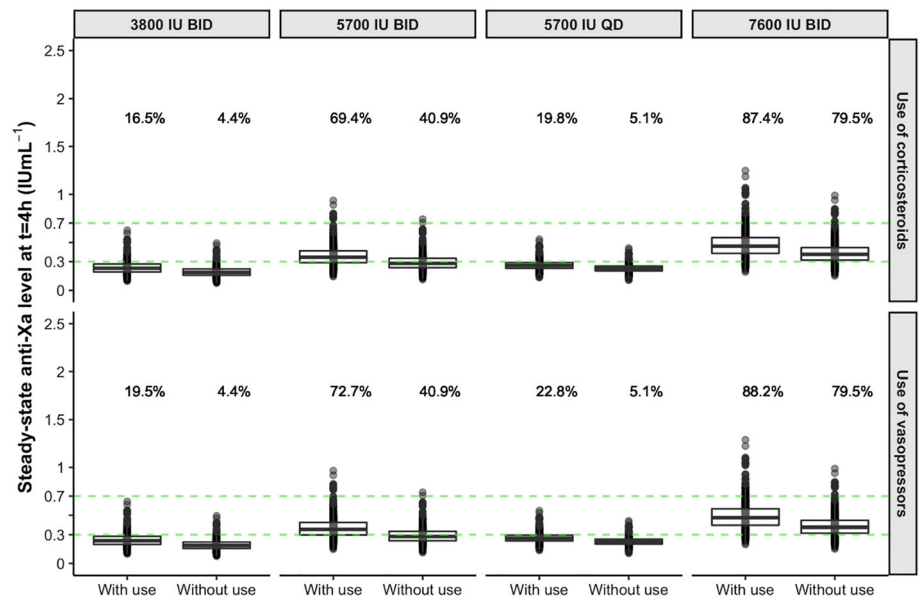


FIGURE 5 Influence of all the continuous covariate relationships taken into account from the final model using Monte Carlo simulations for different dosing strategies

FIGURE 6 Influence of the dichotomous covariate relationships (with vs. without use) taking all covariates into account from the final model using Monte Carlo simulations for different dosing strategies



7600 IU achieved the highest number of anti-Xa levels within the prespecified anti-Xa target level range. In the scenarios where only a single covariate relationship was allowed to differ, the highest number of steady-state $t = 4$ h anti-Xa levels within the prespecified anti-Xa target level range was obtained with 7600 IU BID (Figure S5). Moreover, for each of the dosing strategies the calculated anti-Xa levels were lower as compared with the scenario in which all covariate relationships contributed to the calculation of the individual PK parameter CL. This is due to both dichotomous covariate relationships not being taken into account in the latter scenario. This is exemplified in Figure S6, as the anti-Xa levels obtained when the dichotomous covariate relationships

are taken into account were lower than the anti-Xa levels obtained when all covariate relationships are taken into account. However, the latter lead to higher numbers of anti-Xa levels within the prespecified anti-Xa target level range. Furthermore, the highest number of anti-Xa levels within the prespecified anti-Xa target level range was obtained for the 5700 IU BID and 7600 IU BID dosing regimens. For the assessment of the influence of the covariate relationships on the nadroparin dosing regimen (Figure S7), only CKD-EPI-eGFR demonstrated to be of influence: patients in which a high renal clearance was estimated, a higher dose of nadroparin was necessary in order to achieve an estimated anti-Xa level of 0.4 IU/mL.

4 | DISCUSSION

In this study, a population PK model was constructed using data from critically ill ICU COVID-19 patients receiving thromboprophylactic treatment using nadroparin BID with IIV obtained only for CL. In the covariate analysis, a significant improvement of the model describing the measured anti-Xa levels was obtained by adding inflammation and thrombosis-related parameters, namely, CRP, use of corticosteroids and D-dimer. Furthermore, vasopressor and corticosteroid use significantly decreased CL by 25.1 and 22.5%, respectively. In addition, the most adequate dosing regimen for achieving a target anti-Xa level (0.3–0.7 IU/mL) was evaluated by Bayesian forecasting and Monte Carlo simulation. Using both methods, 5700 IU BID was demonstrated to be the most adequate dosing regimen for the assessed scenarios.

In an earlier population PK analysis, total body weight and lean body weight were covariate relationships associated to CL.²⁵ In addition, their estimate for CL (1380 mL/h/70 kg) was different from CL estimated in the current study (2230 mL/h). As stated earlier, the study included more morbidly obese (BMI > 40 kg/m²) patients ($n = 28$) in comparison with the current cohort ($n = 5$). Moreover, as inflammation-related parameters increase CL, the difference between the estimates could be obtained due to patients having an infection as in our cohort. To our knowledge, other population PK analyses with anti-Xa levels in critically ill patients afflicted by non-COVID-19 infectious disease receiving LMWHs are not available.

Use of CKD-EPI-eGFR as an estimator of renal clearance for ICU patients showed a significant improvement in the constructed model but is known to have limitations.³⁶ It was hypothesized that an important part of nadroparin clearance is not accounted for by association of CKD-EPI-eGFR to CL, specifically in the case of augmented renal clearance associated with COVID-19 induced inflammation.¹⁷ However, the latter was taken into account by the addition of CRP and D-dimer as covariate relationships associated with CL in the constructed model. Moreover, in the covariate analysis, first an exponential relationship between CKD-EPI-eGFR and CL was obtained. However, the association between CKD-EPI-eGFR and CL was more appropriately described by applying a power function, which allowed a better description of the measured anti-Xa levels from the validation cohort. Therefore, CKD-EPI-eGFR was included as a power relationship instead, also taking into account the physiological renal clearance of nadroparin.

In the constructed model, vasopressor use allowed to decrease CL by 25.1%. In an earlier study in critically ill ICU patients using LMWHs, the vasopressor use was associated with a lower concentration of measured anti-Xa levels.¹⁴ This finding is contradictory to the results from the current study, as a decreased clearance was found to result in higher anti-Xa levels. However, only low doses of vasopressors were applied in the current study, usually not exceeding more than approximately 0.1 µg/kg/min. Another explanation could be that vasopressor use is associated with a shock state, resulting in renal hypoperfusion and, thus, necessitating the administration of vasopressors in COVID-19 patients.

The literature concerning the clearance of nadroparin in critically ill COVID-19 patients is scarce. In the present study, it is

demonstrated that COVID-19-related inflammation led to a significant change in CL, resulting in the need for a different thromboprophylactic dosing regimen than in non-COVID-19 ICU patients. The latter is exemplified by a study in which anti-Xa sampling in 16 COVID-19 ICU patients at $t = 4$ h twice weekly was performed, 2 weeks after the start of 5700 IU BID of nadroparin (or 7600 IU BID if total body weight >120 kg).³⁷ In these patients, median (interquartile range) $t = 4$ h anti-Xa levels of 0.38 IU/mL (0.38–0.58) were measured. Furthermore, peak anti-Xa levels were not associated with body weight in this study and 6 patients received CVVH during their ICU stay and mortality nor VTE was reported. Similarly to the current study, $t = 4$ h anti-Xa levels were obtained within the prespecified $t = 4$ h target level range (0.3–0.7 IU/mL) from the current study. Therefore, the dosing regimen proposed in the current study (5700 IU BID) resulted in adequate anti-Xa levels for other studies as well.

The optimal anti-Xa target level range for LMWHs as thromboprophylaxis in critically ill COVID-19 patients has yet to be determined, with current literature assessing different but comparable target ranges. In a first study, the effects of 2 nadroparin dose regimens in combination with imaging for deep venous thrombosis were assessed in a study with critically ill COVID-19 patients. In the standard procedure group, 46 patients received 2850 IU once daily of nadroparin without anti-Xa monitoring.³⁸ In the intervention group, 26 patients received twice-weekly ultrasonography screening and anti-Xa level ($t = 4$ h) tailored administration of nadroparin starting at 3800 IU BID. Significant decreases in 1-month mortality (from 30.4 to 3.85%), use of continuous renal replacement therapy (from 30.4 to 3.85%) and incidence of venous thrombo-embolism (from 41.3 to 15.4%) were demonstrated. However, other factors such as the effect of change in management (i.e., difference in application of ventilation or dexamethasone) of these patients also could have influenced the outcomes in these patients. In a second study, anti-Xa levels were measured twice weekly at $t = 4$ h.³⁹ Clinical outcome was assessed in 56 sub-ICU patients receiving LMWHs with anti-Xa target level range set to 0.3–0.7 IU/mL. Immediately adjusting LMWH dose according to anti-Xa level after correction for mortality-associated factors (e.g., age, use of corticosteroids) lead to a significantly lower risk of COVID-19-related death (adjusted odds ratio 0.04 [95% confidence interval 0.002–0.9; $P = .043$]). Both studies suggest that an anti-Xa target level range, in which the constructed model performs adequately, lowers morbidity and mortality in critically ill COVID-19 patients. However, these studies were not randomized controlled trials and more research is required to determine the relation between anti-Xa levels and clinical outcomes (e.g., mortality, thrombo-embolic and bleeding events).

This study has limitations. Although the parameters of the final model could be accurately estimated, the model was constructed on data from a rather small number of patients. Moreover, no IIV could be quantified for the absorption rate and volume of distribution parameters. Therefore, no covariate relationships could be assessed for these PK parameters. The latter may have decreased the precision for the estimation of the measured anti-Xa levels by the constructed population PK model, as vasopressor use might influence the

microvasculature at the site of absorption. This is exemplified by a study in which a negative correlation ($r = -.68$) between area under the curve was obtained for subcutaneous nadroparin administration and norepinephrine use.⁴⁰ However, other population PK analyses of LMHWs in literature also did not obtain an estimate of IIV for these parameters.^{41,42} Furthermore, the model was constructed based on limited sampling data. The latter may have influenced the estimation of the model parameter.

Next to a modelling cohort, also a validation cohort of patients was used to demonstrate the validity of the constructed model. As anti-Xa levels measured in critically ill COVID-19 patients can be adequately described by the established model, this model could be used for dose individualization. To perform dose individualization, anti-Xa levels can be obtained from routine clinical practice. Using Bayesian forecasting, individual PK parameter estimates can then be obtained to calculate the dose needed to achieve a prespecified anti-Xa target level. Of course, when values for the covariate relationships from the established model are taken into account during Bayesian forecasting, further individualization of the calculated dose can be achieved. Although a validation cohort has been applied to verify whether the model performed adequately, the feasibility of dose individualization in clinical practice should be verified using external validation. In addition, the underlying mechanisms of the obtained covariate relationships should be further investigated in future studies.

COMPETING INTERESTS

L.G.R.R. received the Young Investigators Award 2020 and a travel grant (2019) from Sobi. M.J.H.A.K. has received an unrestricted research grant by Sobi, ZonMw and the Erasmus MC (institutional grant) with all payments directly made to the Department of Hematology of the Erasmus MC (institution). M.J.H.A.K. has received a speaker's fee from Sobi, Roche and Bristol Myers Squibb with all payments directly made to the Department of Hematology of the Erasmus MC (institution). N.G.M.H., T.P. and H.E. have no interests to report.

CONTRIBUTORS

L.G.R.R. and T.P. wrote the manuscript and analysed the results. T.P. performed the population PK analysis. N.G.M.H., M.J.H.A.K. and H.E. supervised the study and gave critical guidance. L.G.R.R. performed data collection. All authors contributed substantially to the writing and critically revised the manuscript, with approval of the final draft.

DATA AVAILABILITY STATEMENT

The datasets used and/or analysed during the current study are available on reasonable request.

ORCID

Lorenzo G. R. Romano  <https://orcid.org/0000-0003-0348-658X>

Nicole G. M. Hunfeld  <https://orcid.org/0000-0001-6856-7028>

Marieke J. H. A. Kruip  <https://orcid.org/0000-0002-0265-4871>

Tim Preijers  <https://orcid.org/0000-0001-6953-0358>

REFERENCES

- Wiersinga WJ, Rhodes A, Cheng AC, Peacock SJ, Prescott HC. Pathophysiology, transmission, diagnosis, and treatment of coronavirus disease 2019 (COVID-19): a review. *JAMA*. 2020;324(8):782-793. doi:10.1001/jama.2020.12839
- Al-Samkari H, Karp Leaf RS, Dzik WH, et al. COVID-19 and coagulation: bleeding and thrombotic manifestations of SARS-CoV-2 infection. *Blood*. 2020;136(4):489-500. doi:10.1182/blood.202006520
- Tang N, Li D, Wang X, Sun Z. Abnormal coagulation parameters are associated with poor prognosis in patients with novel coronavirus pneumonia. *J Thromb Haemost*. 2020;18(4):844-847. doi:10.1111/jth.14768
- Klok FA, Kruip M, van der Meer NJM, et al. Incidence of thrombotic complications in critically ill ICU patients with COVID-19. *Thromb Res*. 2020;191:145-147. doi:10.1016/j.thromres.2020.04.013
- Nahum J, Morichau-Beauchant T, Daviaud F, et al. Venous thrombosis among critically ill patients with coronavirus disease 2019 (COVID-19). *JAMA Netw Open*. 2020;3(5):e2010478. doi:10.1001/jamanetworkopen.2020.10478
- Santoliquido A, Porfida A, Nesci A, et al. Incidence of deep vein thrombosis among non-ICU patients hospitalized for COVID-19 despite pharmacological thromboprophylaxis. *J Thromb Haemost*. 2020;18(9):2358-2363. doi:10.1111/jth.14992
- Helms J, Tacquard C, Severac F, et al. High risk of thrombosis in patients with severe SARS-CoV-2 infection: a multicenter prospective cohort study. *Intensive Care Med*. 2020;46(6):1089-1098. doi:10.1007/s00134-020-06062-x
- Klok FA, Kruip M, van der Meer NJM, et al. Confirmation of the high cumulative incidence of thrombotic complications in critically ill ICU patients with COVID-19: an updated analysis. *Thromb Res*. 2020;191:148-150. doi:10.1016/j.thromres.2020.04.041
- Spyropoulos AC, Levy JH, Ageno W, et al. Scientific and Standardization Committee communication: clinical guidance on the diagnosis, prevention, and treatment of venous thromboembolism in hospitalized patients with COVID-19. *J Thromb Haemost*. 2020;18(8):1859-1865. doi:10.1111/jth.14929
- Panigada M, Bottino N, Tagliabue P, et al. Hypercoagulability of COVID-19 patients in intensive care unit: a report of thromboelastography findings and other parameters of hemostasis. *J Thromb Haemost*. 2020;18(7):1738-1742. doi:10.1111/jth.14850
- Conway EM, Mackman N, Warren RQ, et al. Understanding COVID-19-associated coagulopathy. *Nat Rev Immunol*. 2022;22(10):639-649. doi:10.1038/s41577-022-00762-9
- Roberts JA, Abdul-Aziz MH, Lipman J, et al. Individualised antibiotic dosing for patients who are critically ill: challenges and potential solutions. *Lancet Infect Dis*. 2014;14(6):498-509. doi:10.1016/S1473-3099(14)70036-2
- Xu S-W, Ilyas I, Weng J-p. Endothelial dysfunction in COVID-19: an overview of evidence, biomarkers, mechanisms and potential therapies: 1-15. *Acta Pharmacol Sin*. 2022. doi:10.1038/s41401-022-00998-0
- Dörffler-Melly J, de Jonge E, Pont AC, et al. Bioavailability of subcutaneous low-molecular-weight heparin to patients on vasopressors. *Lancet*. 2002;359(9309):849-850.
- Beunders R, van de Wijgert IH, van den Berg M, van der Hoeven JG, Abdo WF, Pickkers P. Late augmented renal clearance in patients with COVID-19 in the intensive care unit. A prospective observational study. *J Crit Care*. 2021;64:7-9. doi:10.1016/j.jcrc.2021.02.009
- Tomasa-Irriguible TM, Martínez-Vega S, Mor-Marco E, Herraiz-Ruiz A, Ragner-Pardo L, Cubells-Larrosa C. Low molecular weight heparins in COVID-19 patients: beware of augmented renal clearance! *Crit Care*. 2020;24(1):325. doi:10.1186/s13054-020-03058-3
- Udy AA, Roberts JA, Lipman J. Implications of augmented renal clearance in critically ill patients. *Nat Rev Nephrol*. 2011;7(9):539-543. doi:10.1038/nrneph.2011.92

18. Investigators A, Investigators AC-A, Investigators R-C, et al. Therapeutic anticoagulation with heparin in noncritically ill patients with Covid-19. *N Engl J Med*. 2021;385(9):790-802. doi:[10.1056/NEJMoa2105911](https://doi.org/10.1056/NEJMoa2105911)
19. Investigators I, Sadeghipour P, Talasz AH, et al. Effect of intermediate-dose vs standard-dose prophylactic anticoagulation on thrombotic events, extracorporeal membrane oxygenation treatment, or mortality among patients with COVID-19 admitted to the intensive care unit: the INSPIRATION Randomized Clinical Trial. *JAMA*. 2021;325(16):1620-1630. doi:[10.1001/jama.2021.4152](https://doi.org/10.1001/jama.2021.4152)
20. Garcia DA, Baglin TP, Weitz JI, Samama MM. Parenteral anticoagulants: Antithrombotic Therapy and Prevention of Thrombosis, 9th ed: American College of Chest Physicians Evidence-Based Clinical Practice Guidelines. *Chest*. 2012;141(2 Suppl):e24S-e43S. doi:[10.1378/chest.11-2291](https://doi.org/10.1378/chest.11-2291)
21. NIV. Antitrombotisch beleid [Guideline in Dutch]. 2020.
22. Mould DR, Upton RN. Basic concepts in population modeling, simulation, and model-based drug development. *CPT Pharmacometrics Syst Pharmacol*. 2012;1(9):e6. doi:[10.1038/psp.2012.4](https://doi.org/10.1038/psp.2012.4)
23. Jelliffe RW, Schumitzky A, Van Guilder M, et al. Individualizing drug dosage regimens: roles of population pharmacokinetic and dynamic models, Bayesian fitting, and adaptive control. *Ther Drug Monit*. 1993;15(5):380-393. doi:[10.1097/00007691-199310000-00005](https://doi.org/10.1097/00007691-199310000-00005)
24. Laporte S, Mismetti P, Piquet P, Doubine S, Touchot A, Decousus H. Population pharmacokinetic of nadroparin calcium (Fraxiparine®) in children hospitalised for open heart surgery. *Eur J Pharm Sci*. 1999;8(2):119-125. doi:[10.1016/S0928-0987\(98\)00064-5](https://doi.org/10.1016/S0928-0987(98)00064-5)
25. Diepstraten J, Janssen EJ, Hackeng CM, et al. Population pharmacodynamic model for low molecular weight heparin nadroparin in morbidly obese and non-obese patients using anti-Xa levels as endpoint. *Eur J Clin Pharmacol*. 2015;71(1):25-34. doi:[10.1007/s00228-014-1760-4](https://doi.org/10.1007/s00228-014-1760-4)
26. NIV, NHG. Multidisciplinaire richtlijn Chronische nierschade [Guideline in Dutch]. 2018.
27. Bauer RJ. NONMEM Tutorial Part I: description of commands and options, with simple examples of population analysis. *CPT Pharmacometrics Syst Pharmacol*. 2019;8(8):525-537. doi:[10.1002/psp4.12404](https://doi.org/10.1002/psp4.12404)
28. Ahn JE, Karlsson MO, Dunne A, Ludden TM. Likelihood based approaches to handling data below the quantification limit using NONMEM VI. *J Pharmacokinet Pharmacodyn*. 2008;35(4):401-421. doi:[10.1007/s10928-008-9094-4](https://doi.org/10.1007/s10928-008-9094-4)
29. Bauer RJ. NONMEM Tutorial Part II: estimation methods and advanced examples. *CPT Pharmacometrics Syst Pharmacol*. 2019;8(8):538-556. doi:[10.1002/psp4.12422](https://doi.org/10.1002/psp4.12422)
30. Keizer RJ, Karlsson MO, Hooker A. Modeling and simulation workbench for NONMEM: tutorial on Pirana, PsN, and Xpose. *CPT Pharmacometrics Syst Pharmacol*. 2013;2(6):e50.
31. Lindbom L, Ribbing J, Jonsson EN. Perl-speaks-NONMEM (PsN)—a Perl module for NONMEM related programming. *Comput Methods Programs Biomed*. 2004;75(2):85-94. doi:[10.1016/j.cmpb.2003.11.003](https://doi.org/10.1016/j.cmpb.2003.11.003)
32. Hutmacher MM, Kowalski KG. Covariate selection in pharmacometric analyses: a review of methods. *Br J Clin Pharmacol*. 2015;79(1):132-147. doi:[10.1111/bcp.12451](https://doi.org/10.1111/bcp.12451)
33. Karlsson MO, Savic RM. Diagnosing model diagnostics. *Clin Pharmacol Ther*. 2007;82(1):17-20. doi:[10.1038/sj.clpt.6100241](https://doi.org/10.1038/sj.clpt.6100241)
34. Bergstrand M, Hooker AC, Wallin JE, Karlsson MO. Prediction-corrected visual predictive checks for diagnosing nonlinear mixed-effects models. *AAPS J*. 2011;13(2):143-151. doi:[10.1208/s12248-011-9255-z](https://doi.org/10.1208/s12248-011-9255-z)
35. Bonate PL. A brief introduction to Monte Carlo simulation. *Clin Pharmacokinet*. 2001;40(1):15-22. doi:[10.2165/00003088-200140010-00002](https://doi.org/10.2165/00003088-200140010-00002)
36. Sunder S, Jayaraman R, Mahapatra HS, et al. Estimation of renal function in the intensive care unit: the covert concepts brought to light. *J Intensive Care*. 2014;2(1):31. doi:[10.1186/2052-0492-2-31](https://doi.org/10.1186/2052-0492-2-31)
37. Vlot EA, Van den Dool EJ, Hackeng CM, Sohne M, Noordzij PG, Van Dongen EPA. Anti Xa activity after high dose LMWH thrombosis prophylaxis in covid 19 patients at the intensive care unit. *Thromb Res*. 2020;196:1-3. doi:[10.1016/j.thromres.2020.07.035](https://doi.org/10.1016/j.thromres.2020.07.035)
38. Stessel B, Vanvuchelen C, Bruckers L, et al. Impact of implementation of an individualised thromboprophylaxis protocol in critically ill ICU patients with COVID-19: a longitudinal controlled before-after study. *Thromb Res*. 2020;194:209-215. doi:[10.1016/j.thromres.2020.07.038](https://doi.org/10.1016/j.thromres.2020.07.038)
39. Trunfio M, Salvador E, Cabodi D, et al. Anti-Xa monitoring improves low-molecular-weight heparin effectiveness in patients with SARS-CoV-2 infection. *Thromb Res*. 2020;196:432-434. doi:[10.1016/j.thromres.2020.09.039](https://doi.org/10.1016/j.thromres.2020.09.039)
40. Cihlar R, Sramek V, Papiez A, Penka M, Suk P. Pharmacokinetic comparison of subcutaneous and intravenous nadroparin administration for thromboprophylaxis in critically ill patients on vasopressors. *Pharmacology*. 2020;105(1-2):73-78. doi:[10.1159/000502847](https://doi.org/10.1159/000502847)
41. van der Heijden C, Ter Heine R, Kooistra EJ, et al. Effects of dalteparin on anti-Xa activities cannot be predicted in critically ill COVID-19 patients. *Br J Clin Pharmacol*. 2022;88(6):2982-2987. doi:[10.1111/bcp.15208](https://doi.org/10.1111/bcp.15208)
42. Zufferey PJ, Dupont A, Lanoiselée J, et al. Pharmacokinetics of enoxaparin in COVID-19 critically ill patients. *Thromb Res*. 2021;205:120-127. doi:[10.1016/j.thromres.2021.07.010](https://doi.org/10.1016/j.thromres.2021.07.010)

SUPPORTING INFORMATION

Additional supporting information can be found online in the Supporting Information section at the end of this article.

How to cite this article: Romano LGR, Hunfeld NGM, Kruij MJHA, Endeman H, Preijers T. Population pharmacokinetics of nadroparin for thromboprophylaxis in COVID-19 intensive care unit patients. *Br J Clin Pharmacol*. 2022;1-12. doi:[10.1111/bcp.15634](https://doi.org/10.1111/bcp.15634)